Orientation and Bonding of 4,4′-Biphenyldiisocyanide

A. N. Caruso,[†] R. Rajesh,[‡] G. Gallup,[†] J. Redepenning,[‡] and P. A. Dowben*,[†]

Department of Physics and Astronomy and the Center for Materials Research and Analysis, Behlen Laboratory of Physics, University of Nebraska—Lincoln, Lincoln, Nebraska 68588-0111, and Department of Chemistry, Hamilton Hall, University of Nebraska—Lincoln, Lincoln, Nebraska 68588-0304

Received: December 4, 2003; In Final Form: April 8, 2004

The orientation and bonding of 4,4′-biphenyldiisocyanide (BPDI) adsorbed by solution on Au(111) has been examined by polarization dependent photoemission and inverse photoemission. The highest occupied molecular orbital to lowest unoccupied molecular orbital gap for BPDI is about 10.8 eV, with the Fermi level nearly midgap. The electronic structure of isocyano-functionalized polyphenyls suggests that they are better dielectrics than thiol-functionalized polyphenyls.

Thiol-functionalized (H−S) molecules such as oligobenzenethiols and alkanethiols have received considerable attention because of their promise as materials for molecular electronics.[1−19] Highly ordered molecular layers are sought, ideally with the long molecular axis along surface normal, perhaps aided by the thiol functional groups. In addition, voltage dependent hysteresis along the large conductance channels would provide additional device functionality. The reality of the thiol-functionalized molecules is that strong Au−S bonds often form but the bonding orientation of the long molecular axis is rarely along the surface normal. This can lead to a number of complications[20,21] including imperfections and disorder within the molecular layer, not to mention polycrystalline molecular layers.

Nitrile[22] and isocyano[23−27] end groups offer an alternative means for attaching phenyl based molecules to metals. Furthermore, isocyano end groups appear to offer lower thermionic barriers to conduction.[23−24] For these reasons we studied the orientation, bonding, and electronic properties of 4,4′-biphenyldiisocyanide (BPDI), adsorbed from solution on Au(111). We provide some comparisons with the results obtained from the related biphenyldimethylthiol.[21]

Light polarization dependent angle-resolved photoemission experiments were carried out using synchrotron radiation, dispersed by a 3 m toroidal monochromator, at the Center for Advanced Microstructure and Devices in Baton Rouge, LA, as described elsewhere.[21,28] All angles (both light incidence angles as well as photoelectron emission angles) reported herein are with respect to the substrate surface normal. Because of the highly plane polarized nature of dispersed synchrotron light through the toroidal grating monochromator, large light incidence angles result in a vector potential **A** more parallel to the surface normal (p-polarized light), whereas smaller light incidence angles result in the vector potential **A** residing more in the plane of the surface (s-polarized light). From a comparison of light incidence angle photoemission spectra, the irreducible group representation band symmetries can be assigned using[21,29]

$$\left(\frac{d\sigma}{d\Omega}\right)_{PES} \propto |\langle\Psi_f|\mathbf{A}\cdot\mathbf{p} + \mathbf{p}\cdot\mathbf{A}|\Psi_i\rangle|^2\delta(E_f - E_i - h\nu) \quad (1)$$

In this work, we applied the C_{2v} point group to adsorbed BPDI, due to the symmetry reduction from the D_{2h} point group of gas-phase BPDI. For the photoemission results reported here, the photoelectrons were collected normal to the surface ($\bar{\Gamma}$ or $k_{||} = 0$) to preserve the highest possible point group symmetry. This means that application of equation 1 to the selection rules in photoemission results in molecular orbitals of a_1 symmetry becoming enhanced in p-polarized light whereas b_1 and b_2 symmetry molecular orbitals are enhanced with increasing s-polarized light for adsorbed BPDI. Molecular orbitals of a_2 symmetry are forbidden.

The electronic structure of the unoccupied states was investigated using inverse photoemission spectroscopy (IPES). For the IPES studies, a Geiger−Müller detector with a CaF_2 window was used in conjunction with an Erdman−Zipf electron gun[30] and the overall energy resolution in inverse photoemission was ∼400 meV. For both photoemission and inverse photoemission, binding energies are reported with respect to the substrate Fermi level ($E - E_F$), determined from spectra taken of clean gold and tantalum in intimate contact with the substrate.

The Au(111) substrate surface was prepared by epitaxial growth on Si(111), and verified by X-ray diffraction to possess only the (111) peaks. Deposition of BPDI on the gold substrates was undertaken from solution. These molecular layers were prepared and assembled on gold following the recipe described by Kubiak and co-workers.[26] After deposition, while still in the glovebox, each sample was placed in a sealed container under nitrogen. The sample was exposed to atmosphere only for a short period before placing the sample into the UHV chamber. No evidence was found for photodegradation, local photoinduced thermal desorption, and/or charging during the course of our measurements. For comparison, low coverages of 4,4′-biphenyldiisocyanide (BPDI) were adsorbed from the vapor on clean gold at 140 K. The 4,4′-biphenyldiisocyanide (BPDI) vapor was introduced into the UHV chamber through a standard leak valve.

* Corresponding author. Address: 116 Brace Laboratory, University of Nebraska, P.O. Box 880111, Lincoln, NE 68588-0111. Phone: 402-472-9838. Fax: 402-472-2879. E-mail: pdowben@unl.edu.

[†] Department of Physics and Astronomy and the Center for Materials Research and Analysis, Behlen Laboratory of Physics.

[‡] Department of Chemistry.

10.1021/jp037710m CCC: $27.50
Published on Web 05/12/2004

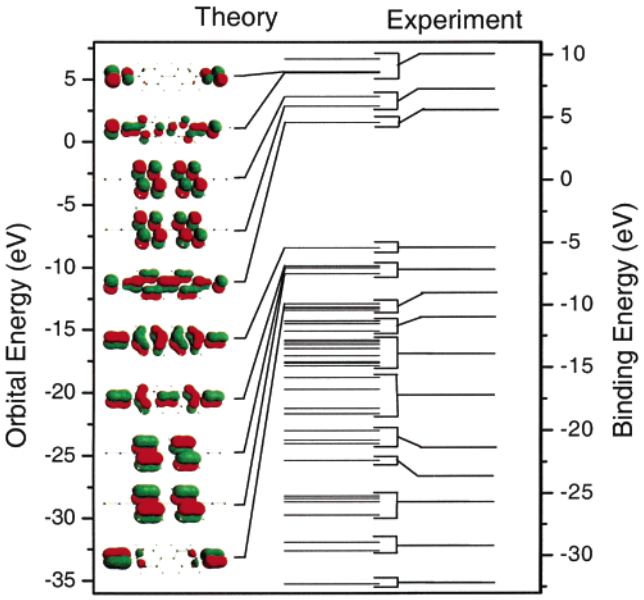

Figure 1. Left: calculated binding energies referenced to the vacuum level with the associated molecular orbital contours. Right: experimental photoemission features grouped to their respective calculated orbitals and referenced to the Fermi level.

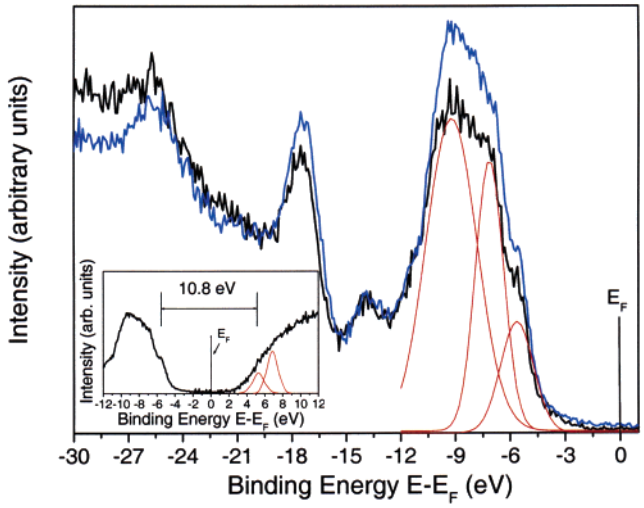

Figure 2. Photoemission spectra taken using 55 eV incident light. Inset: combined photoemission and inverse photoemission of biphenyldiisocyanide, highlighting the experimental band gap, that is nearly centered about the Fermi level. The blue represents p-polarized light, and black is s+p polarized light, showing enhancements with p-polarization.

Calculations to model the biphenyldiisocyanide molecular orbitals were performed using the GAMESS ab initio package.[31] A standard 6-31G(d) basis set was used, and all molecular geometries were optimized at this level. The starting geometries were obtained by assigning the molecule to the D_{2h} point group using standard bond lengths. Several molecular conformations or geometries were considered (vide infra). The highest molecular point group symmetry possible, after adsorption (C_{2v}), does seem to be applicable to the data, as schematically shown in Figure 1.

For the BPDI films deposited from solution, the gold substrate photoemission and inverse photoemission features are completely suppressed (Figure 2). A number of molecular orbitals combine to give rise to a single photoemission or inverse photoemission feature, but on the basis of our calculations all the photoemission and inverse photoemission features can be assigned to biphenyldiisocyanide molecular orbitals as summarized in Figure 1 and Table 1. The suppression of the Au substrate signal, as in previous studies,[21] indicates that the biphenyldiisocyanide film thickness exceeds the photoelectron mean free path of photoelectrons from the substrate (>3 nm thick). The calculated orbital energies are offset from experimental values, which cannot be attributed to the work function.[29] Such offsets are common and have been observed in comparing photoemission with ground state theory of large molecular adsorbates such as adsorbed alkanethiols,[20] metallocenes,[32] poly(vinylidene fluoride),[33] *nido*- and *closo*-carboranes,[21,34] and many others.[29] The difference between ground state theory and experiment may be a result of solid-state effects such as screening but can also occur in the comparison of gas-phase spectra with theory as well,[32,35] as electron spectroscopies, like photoemission, are final state spectroscopies. Final state effects due to photovoltaic charging are not evident in the studies here.

The experimental HOMO (highest occupied molecular orbital) to LUMO (lowest unoccupied molecular orbital) gap can be extracted from combined photoemission and inverse photoemission spectra (inset to Figure 2). The experimental 10.8 eV gap, derived from the vertical HOMO−LUMO band positions, is in close agreement with the 10.0 eV gap expected from theory. Unlike biphenyldimethylthiol, which is clearly an n-type insulator on gold,[21] biphenyldiisocyanide is nearly perfectly compensated, because the position of the Fermi level is near the middle of the experimental HOMO−LUMO gap (inset to Figure 2). Nonetheless, from the observed paucity of states at the Fermi level, both biphenyldiisocyanide and biphenyldimethylthiol are expected to be insulators. The electronic structure evident in photoemission and inverse photoemission for BPDI adsorbed on gold is characteristic of molecules perturbed by adsorption and the substrate, not altered by a true impurity doping effect. Though the relative placement of the molecular orbitals with respect to the Fermi level cannot be taken as an infallible guide as to the majority carrier, such band offset characteristics, nonetheless, have been shown to be consistent with some molecular electronic device characteristics.[36−38]

The experimental HOMO to LUMO gap of about 10.8 eV for biphenyldiisocyanide is substantially larger than the HOMO−LUMO gap for biphenyldimethylthiol similarly determined (7.8 eV).[21] The theoretical HOMO−LUMO gaps are similar for both biphenyldiisocyanide and biphenyldimethylthiol, at 10.65 and 10.33 eV, respectively. The difference between theory and experiment suggests that the charge donation from the metal substrate toward biphenyldimethylthiol is more significant than for biphenyldiisocyanide, consistent with the differences in electron affinities between H−S- and C═N− groups.

The strong polarization dependence shown in Figure 2 indicates that there is a preferential orientation and self-assembly of the BPDI. This evidence indicates that defect presence is limited to vacancies formed from the inherent self-assembly. However, photoemission and inverse photoemission reveal no defect like states in the large HOMO−LUMO gap. Hence, we feel that whatever the imperfections in our films, the band gap determination is substantively affected, but the same may not be true of all measurements.

Using molecular conductance spectroscopy, Hong et al.[25] reported that the highest occupied molecular orbital to Fermi level gap is 0.53 eV for biphenyldiisocyanide. From this value, we may infer that the HOMO to LUMO gap is approximately 1.1 eV, assuming that the chemical potential is midgap. Indeed, molecular conductance spectroscopy suggests that the HOMO

TABLE 1: Calculated Orbital Energies Referenced to the Vacuum Level in the Gas Phase with the Respective Irreducible Symmetry Representations from the D_{2h} Point Group[a]

	calcd orbital energies (eV)	exptl binding energies $E - E_F$ (eV)	D_{2h} symmetry MOs	C_{2v} symmetry		
				MOs in (1)	MOs in (2)	MOs in (3)
LUMO−5	5.611		b_{1g}	b_1	a_2	b_2
LUMO−4	5.5185	9.91	b_{2u}	b_1	b_2	a_1
LUMO−3	3.6354		b_{2g}	b_2	b_1	a_2
LUMO−2	3.611	7.14	a_u	a_2	a_2	a_2
LUMO−1	2.849	not resolved	b_{3g}	a_2	b_2	b_1
LUMO	1.551	5.33	b_{1u}	b_2	a_1	b_1
HOMO	−8.4246	−5.47	b_{2g}	b_2	b_1	a_2
HOMO+1	−9.8696	forbidden	a_u	a_2	a_2	a_2
HOMO+2	−10.041	−6.94	b_{3g}	a_2	b_2	b_1
HOMO+3	−10.5009		b_{1u}	b_2	a_1	b_1
HOMO+4	−12.9281		a_g	a_1	a_1	a_1
HOMO+5	−12.9336		b_{3u}	a_1	b_1	b_2
HOMO+6	−13.2002	−9.08	b_{1g}	b_1	a_2	b_2
HOMO+7	−13.2547		b_{2g}	b_2	b_1	a_2
HOMO+8	−13.4397		b_{2u}	b_1	b_2	a_1
HOMO+9	−14.2833		b_{1g}	b_1	a_2	b_2
HOMO+10	−14.3268	−11.12	b_{1u}	b_2	a_1	b_1
HOMO+11	−14.5472		a_g	a_1	a_1	a_1
HOMO+12	−15.1078		b_{2u}	b_1	b_2	a_1

[a] Experimental binding energies referenced to the Fermi level with the correlated irreducible symmetry representations from the D_{2h} to C_{2v} point groups for the three possible orientations with a linear molecular geometry: (1) long molecular axis along the surface normal, (2) long molecular axis parallel to the surface with the benzene plane also parallel to the surface, and (3) long molecular axis parallel to the surface with the benzene plane perpendicular to the surface.

to LUMO gap is far smaller for both the mono- and diisocyano-terminated molecular species than for the corresponding monothiol or dithiol species[25] and, in almost all cases, smaller than found from combined photoemission and inverse photoemission studies. This suggests that the gap measured by molecular conductance spectroscopy may be dominated by contributions from the gold substrate, particularly for the occupied states (negative sample bias),[21] but in any case is not a good measure of the HOMO−LUMO gap with this class of molecules. Also, if the molecular film is not a single crystal, filamentary conduction (through the film) could dominate.[20]

The orientation of BPDI was investigated using the light polarization dependent angle-resolved photoemission. As noted above, different combinations of molecular conformation or geometry and orientation of the long molecular axis and benzene ring plane orientation were considered. Each combination yielded a molecular bonding configuration (molecular conformation or geometry and orientation) whose expected light polarization dependence, based on symmetry and selection rules in photoemission, was compared with the experimentally obtained dependence of the photoemission spectra on light polarization (Figure 2). Two molecular geometries were considered with the benzene planes parallel to each other. The molecule is linear in the idealized molecular conformation or geometry with a D_{2h} gas phase point group symmetry, though the molecule must be of a lower symmetry upon adsorption (C_{2v} or lower symmetry). A second molecular conformation or geometry was also considered on the basis of work completed using synthetic analogues,[39−40] with a single bent nitrogen to benzene bond but with the benzene ring planes parallel. Given that a "bent" nitrogen−benzene bond would be likely only as a result of molecular bonds with the substrate, the resulting canted molecular orientation restricts our knowledge of the nitrogen−benzene bond conformation at the other end of the molecule, such that a much reduced symmetry must be assumed for such an adsorbed species. Other low symmetry molecular bonding configurations were also considered.

The light polarization dependent normalized valence band photoemission of BPDI show clear enhancements in p-polarization for the spectral features with contributions from the HOMO through HOMO 8 and HOMO 21 through HOMO 24 molecular orbitals, as seen in Figure 2. This very strong light polarization dependence of almost all the photoemission features due to BPDI suggests that the molecule retains the characteristics of a high point group symmetry in the molecular film. Lower molecular symmetries are therefore unlikely, including situations where benzene ring planes are canted with respect to one another or one or both nitrogen−benzene bonds are "bent", as discussed above. "Bent" nitrogen−benzene bonds can be reconciled with our data if both isocyano ends exhibit the same bond bending, in the same direction, reducing the symmetry to only C_{2v}. "Bending" both nitrogen−benzene bonds is highly unlikely as this distortion is energetically unfavorable.

Thus, we considered three separate adsorption orientations for the linear molecular conformation with coplanar benzene rings. Each placement of the molecular axis and the benzene ring planes reduces the gas-phase D_{2h} group to an adsorbed phase C_{2v} point group symmetry (or lower). These high-symmetry configurations for adsorbed biphenyldiisocyanide are (**1**) long molecular axis along surface normal, (**2**) long molecular axis parallel to surface with benzene plane also parallel to the surface, and (**3**) long molecular axis parallel to surface with benzene plane perpendicular to the surface.

The correlation of irreducible representations, associated with the reduction in symmetry from D_{2h} to C_{2v}, is given in Table 1. The molecular coordinate system (placing the *z*-axis perpendicular to the benzene plane, the *x*-axis parallel to the long molecular axis, and the *y*-axis parallel to the benzene plane but perpendicular to the long molecular axis) is altered with the reduction of symmetry associated with adsorption so that the

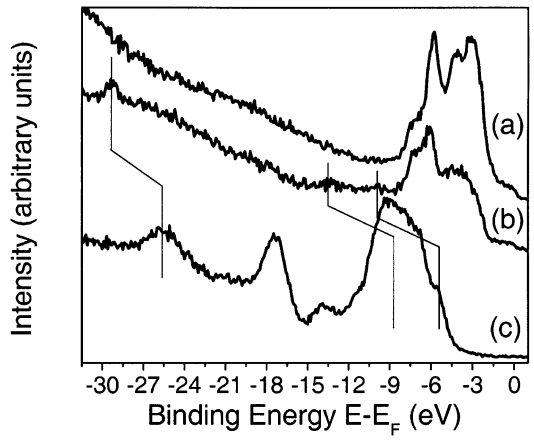

Figure 3. Photoemission spectra taken with p-polarization at 55 eV photon energy: (a) clean Au; (b) vapor deposited 4,4′-biphenyldiisocyanide; (c) solution deposited 4,4′-biphenyldiisocyanide. Notice the much higher binding energies associated with molecular orbitals of BPDI bound to gold in vapor (thin) versus the weaker binding energies for the molecular orbitals of BPDI bound to itself.

z-axis is along the surface normal. Strong enhancement of the photoemission features in p-polarized light with a molecular adsorption configuration (**1**), i.e., with the long molecular axis parallel with the surface normal, is a possible orientation consistent with our data. In view of the data, the configurations with both the molecular axis and the benzene planes parallel with the surface (**2**) is also a possible configuration.

Molecular orbitals of a_2 symmetry are forbidden in both photoemission and inverse photoemission. The clear observation of the highest occupied molecular orbital (HOMO) and the strong combined HOMO+2 and HOMO+3 photoemission feature in p-polarized light tend to exclude any possibility of a bonding configuration for 4,4′-biphenyldiisocyanide with the molecular axis parallel with the surface but with the benzene planes perpendicular (**3**) with the surface. The photoemission feature resulting from the combination occupied molecular orbitals HOMO+4 though HOMO+8, at 9.1 eV binding energy, is enhanced in p-polarized light, whereas the photoemission feature associated with HOMO+9, +10, +11, and +12 is not. From selection rules (eq 1) this slightly favors an orientation with the long molecular axis of 4,4′-biphenyldiisocyanide placed parallel with the surface normal.

Reflection absorption infrared spectroscopy (RAIR) of 4,4′-biphenyldiisocyanide on Au(111) was interpreted[26] as providing evidence that the long molecular axis is parallel with the surface normal, i.e., configuration **1**, in agreement with our photoemission results. Unfortunately, other BPDI bonding configurations might also lead to the same reflection absorption infrared spectroscopy results. These bonding configurations include placing the long axis of 4,4′-biphenyldiisocyanide nearly parallel with the surface, but with the C═N− group slightly bent so as to bond with the substrate. Thicker BPDI molecular films in which some (but not all) of the isocyano groups directly bond to the surface might also provide the observed RAIRS results. The precise orientation of the biphenyldiisocyanide molecular species at the gold interface, for our thicker (>3 nm) BPDI films deposited from solution, cannot be determined from the data presented here due to the limited photoelectron mean free path.

Because there is no evidence of photovoltaic charging (leading to large apparent increases in binding energy) for our BPDI films on gold, photoemission spectra of biphenyldiisocyanide on Au(111), adsorbed from vapor (Figure 3b) and deposited from solution (Figure 3c) can be compared. For the BPDI adsorbed on gold from the vapor, a few photoemission features attributable to the biphenyldiisocyanide molecular orbitals can be distinguished from the gold substrate photoemission features. It is difficult to assign the molecular orbitals to the photoemission features observed when the 4,4′-biphenyldiisocyanide is adsorbed on gold from the vapor, due the possibility that the highest occupied molecular orbital is obscured by the gold substrate 5d photoemission features. The most reasonable assignment (indicated in Figure 3) based upon the molecular orbital configuration suggests that there is a difference in binding energies, of approximately 3.5 eV, between the molecular orbital photoemission features observed for molecular adsorption from the vapor (Figure 3b) and deposition from solution (Figure 3c). The higher binding energies for the BPDI-induced photoemission features, resulting from adsorption on gold from the vapor, demonstrates that extramolecular bonding of BPDI to itself is much weaker than BPDI to the substrate. Unless the BPDI thin film samples, examined using RAIRS,[26] are shown to be a single molecular monolayer, interpretation of the RAIRS spectra will be difficult.

We have shown that BPDI adsorbed from solution on Au(111) bonds with the long molecular axis parallel to the surface normal, although an orientation with the long molecular axis parallel with the surface and the benzene ring planes also parallel (**2**), cannot be conclusively eliminated. In this regard, the orientation appears to resemble the assignment derived from RAIRS,[26] but with some limitations in the orientation assignment due to the multiple contributions to each photoemission feature.

We find that the calculated theoretical HOMO−LUMO gap for BPDI is very similar to the analogous dithiols. The experimental gap for BPDI, at 10.8 eV derived from combined photoemission and inverse photoemission results, is much larger than the experimental HOMO−LUMO gap obtained for the biphenyldimethylthiol at 7.8 eV. Furthermore, the Fermi level placement, within the HOMO−LUMO gap, suggests that adsorbed multilayers of biphenyldimethylthiol are more n-type than are multilayer films of biphenyldiisocyanide. BPDI exhibits a larger barrier to thermionic conduction due to the larger gap between the LUMO and the Fermi level ($E_{LUMO} - E_F$) and therefore should be a better dielectric than many oligobenzenethiols. The experimental results here differ from previous measurements[23−25] that suggest a smaller HOMO−LUMO gap for biphenyldiisocyanide than biphenyldimethylthiol. Previous measurements of the HOMO−LUMO gap[23−25] may suffer from a number of experimental problems including, but not limited to, sample imperfections.

Acknowledgment. This work was supported by the National Science Foundation through the NSF "QSPINS" MRSEC (DMR 0213808), the Office of Naval Research, and the Nebraska Research Initiative.

References and Notes

(1) Heath, J. A.; Ratner, M. A. *Phys. Today* **2003**, 43.

(2) Aviram, A.; Ratner, M. A. *Chem. Phys. Lett.* **1994**, *29*, 277.

(3) Martin, A. S.; Sambles, J. R.; Ashwell. G. *Phys. Rev. Lett.* **1994**, *70*, 218.

(4) Howell, S.; Kuila, D.; Kasibhatla, B.; Kubiak, C. P.; Janes, D.; Reifenberger, R. *Langmuir* **2002**, *18*, 5120−5125.

(5) Janes, D. B.; Lee, T.; Liu, J.; Batistuta, M.; Chen, N. P.; Walsh, B. L.; Andres, R. P.; Chen, E. H.; Melloch, M. R.; Woodall, J. M.; Reifenberger, R. *J. Electron. Mater.* **2000**, *29*, 565−569.

(6) Janes, D. B.; Batistuta, M.; Datta, S.; Melloch, M. R.; Andres, R. P.; Liu, J.; Chen, N. P.; Lee, T.; Reifenberger, R.; Chen, E. H.; Woodall, J. M. *Superlattices Microstruct.* **2000**, *27*, 555−563.

(7) Tian, W. D.; Datta, S.; Hong, S. H.; Reifenberger, R.; Henderson, J. I.; Kubiak, C. P. *J. Chem. Phys.* **1998**, *109*, 2874−2882.

(8) Wang, W. Y.; Lee, T.; Reed, M. A. *Phys. Rev. B* **2003**, *68*, Art. No. 035416.

(9) Wang, W. Y.; Lee, T.; Reed, M. A. *Physica E* **2003**, *19*, 117−125.

(10) Chen, J.; Su, J.; Wang, W.; Reed, M. A. *Physica E* **2003**, *16*, 17−23.

(11) Tour, J. M.; Rawlett, A. M.; Kozaki, M.; Yao, Y. X.; Jagessar, R. C.; Dirk, S. M.; Price, D. W.; Reed, M. A.; Zhou, C. W.; Chen, J.; Wang, W. Y.; Campbell, I. *Eur. J. Chem. A* **2001**, *7*, 5118−5134.

(12) Robertson, N.; McGowan, C. A. *Chem. Soc. Rev.* **2003**, *32*, 96−103.

(13) Fan, F. R. F.; Yang, J. P.; Cai, L. T.; Price, D. W.; Dirk, S. M.; Kosynkin, D. V.; Yao, Y. X.; Rawlett, A. M.; Tour, J. M.; Bard, A. J. *J. Am. Chem. Soc.* **2002**, *124*, 5550−5560.

(14) Reed, M. A. *MRS Bull.* **2001**, *26*, 113−120.

(15) Reed, M. A.; Zhou, C.; Muller, C. J.; Burgin, T. P.; Tour, J. M. *Science* **1997**, *278*, 252−254.

(16) Bumm, L. A.; Arnold, J. J.; Cygan, M. T.; Dunbar, T. D.; Burgin, T. P.; Jones, L.; Allara, D. L.; Tour, J. M.; Weiss, P. S. *Science* **1996**, *271*, 1705−1707.

(17) Schön, J. H.; Meng, H.; Bao, Z. *Nature* **2001**, *413*, 713.

(18) Schön, J. H.; Meng, H.; Bao, Z. *Science* **2001**, *294*, 2138.

(19) Datta, S.; Tian, W.; Hong, S.; Reifenberger, R.; Henderson, J. I.; Kubiak, C. P. *Phys. Rev. Lett.* **1997**, *79*, 2530.

(20) Ovchenkov, Y. A.; Geisler, H.; Burst, J. M.; Thornburg, S. N.; Ventrice, C. A., Jr.; Zhang, C.; Redepenning, J.; Losovyj, Y.; Rosa, L.; Dowben, P. A.; Doudin, B. *Chem. Phys. Lett.* **2003**, *381*, 7−13 and references therein.

(21) Caruso, A. N.; Rajesekaran, R.; Gallup, G.; Redepenning, J.; Dowben, P. A. *J. Phys.: Condens. Matter* **2004**, *16*, 845−860.

(22) Dirk, S. M.; Tour, J. M. *Tetrahedron* **2003**, *59*, 287−293.

(23) Chen, J.; Wang, W.; Klemic, J.; Reed, M. A.; Axelrod, B. W.; Kaschak, D. M.; Rawlett, A. M.; Price, D. W.; Dirk, S. M.; Tour, J. M.; Grubisha, D. S.; Bennett, D. W. *Ann. N. Y. Acad. Sci.* **2002**, *960*, 69−99.

(24) Chen, J.; Calvet, L. C.; Reed, M. A.; Carr, D. W.; Grubisha, D. S.; Bennett, D. W. *Chem. Phys. Lett.* **1999**, *313*, 741−748.

(25) Hong, S.; Reifenberger, R.; Tian, W.; Datta, S.; Henderson, J.; Kubiak, C. P. *Superlattices Microstruct.* **2000**, *28*, 289−303.

(26) Henderson, J. I.; Feng, S.; Bein, T.; Kubiak, C. P. *Langmuir* **2000**, *16*, 6183−6187.

(27) Henderson, J. I.; Feng, S.; Ferrence, G. M.; Bein T.; Kubiak, C. P. *Inorg. Chim. Acta* **1996**, *242*, 115.

(28) Dowben, P. A.; LaGraffe, D.; Onellion, M. *J. Phys. Condens. Matter* **1989**, *1*, 6571.

(29) Dowben, P. A.; Choi, J.; Morikawa, E.; Xu, B. *Handbook of Thin Films, Volume 2: Characterization and Spectroscopy of Thin Films*; Academic Press: New York, 2002; Chapter 2, pp 61−114.

(30) Erdman, P. W.; Zipf, E. C. *Rev. Sci. Instum.* **1982**, *53*, 225−227.

(31) Schmidt, M. W.; Baldridge, K. K.; Boatz, J. A.; Elbert, S. T.; Gordon, M. S.; Jensen, J. H.; Koseki, S.; Matsunaga, N.; Nguyen, K. A.; Su, S. J.; Windus, T. L.; Dupuis, M.; Montomery, J. A. *J. Comput. Chem.* **1993**, *14*, 1347−1363.

(32) Welipitiya, D.; Dowben, P. A.; Zhang, J.; Pai W. W.; Wendelken, J. F. *Surf. Sci.* **1996**, *367*, 20−32. Waldfried, C.; Welipitiya, D.; Hutchings, C. W.; de Silva, H. S. V.; Gallup, G. A.; Dowben, P. A.; Pai, W. W.; Zhang, J.; Wendelken J. F.; Boag, N. M. *J. Phys. Chem. B* **1997**, *101*, 9782−9789. Welipitiya, D.; Borca, C. N.; Waldfried, C.; Hutchings, C.; Sage, L.; Woodbridge, C. M.; Dowben, P. A. *Surf. Sci.* **1997**, *393*, 34−46.

(33) Duan, Chun-gang; Mei, W. N.; Hardy, J. R.; Ducharme, S.; Choi, J.; Dowben, P. A. *Europhys. Lett.* **2003**, *61*, 81−87.

(34) Caruso, A. N.; Bernard, L.; Xu, B.; Dowben, P. A. *J. Phys. Chem. B* **2003**, *107*, 9620−9623. Lee, S.; Li, D.; Dowben, P. A.; Perkins, F. K.; Onellion, M.; Spencer, J. T. *J. Am. Chem. Soc.* **1991**, *113*, 8444−8447. Zhang, J.; McIlroy, D. N.; Dowben, P. A.; Zeng, H.; Vidali, G.; Heskett, D.; Onellion, M. *J. Phys. Cond. Matter* **1995**, *7*, 7185−7194.

(35) Hutchings, C. W.; Hitchcock, A. P.; Wen, A. T.; Hwang, S.-D.; Glass, J. A.; Spencer, J. T.; Hu, Y.-F.; Bancroft, G. M.; Dowben, P. A. *J. Electron. Spectrosc. Relat. Phenom.* **1998**, *94*, 187−194. Hutchings, C. W.; Hwang, S.-D.; Dowben, P. A.; Glass, J. A.; Spencer, J. T.; Hu, Y.-F.; Bancroft, G. M. *Phys. Low Dim. Struct.* **1998**, *1/2*, 65−70. Hitchcock, A. P.; Urquhart, S. G.; Wen, A. T.; Kilcoyne, A. L. D.; Tyliszczak, T.; Rühl, E.; Kosugi, N.; Bozek, J. D.; Spencer, J. T.; McIlroy, D. N.; Dowben, P. A. *J. Phys. Chem. B* **1997**, *101*, 3483−3493. Byun, D.; Lee, S.; Hu, Yong-Feng; Bancroft, G. M.; Hwang, S.; Glass, J. A.; Zhang, J.; Spencer, J. T.; Ma J.; Dowben, P. A. *Journ. Electron Spectrosc. Relat. Phenom.* **1994**, *69*, 111−116. Hitchcock, A. P.; Wen, A. T.; Lee, S.; Glass, J. A.; Spencer, J. T.; Dowben, P. A. *J. Phys. Chem.* **1993**, *97*, 8171−8181.

(36) Xu, B.; Ovchenkov, Y.; Bai, M.; Caruso, A. N.; Sorokin, A. V.; Ducharme, S.; Doudin, B.; Dowben, P. A. *Appl. Phys. Lett.* **2002**, *81*, 4281−4283.

(37) Gao, W.; Kahn, A. *J. Phys. Condens. Matter* **2003**, *15*, S2757.

(38) Gao, W.; Kahn, A. *Org. Electron.* **2002**, *3*, 53.

(39) Adams, R. D.; Cotton, F. A. *Inorg. Chem.* **1974**, *13*, 249−253.

(40) Day, V. W.; Day, R. O.; Kristoff, J. S.; Hirsekorn, F. J.; Muetterties, E. L. *J. Am. Chem. Soc.* **1975**, *97*, 2571−2573.